Köthur, P., Witt, C., Sips, M., Marwan, N., Schinkel, S., Dransch, D. (2015): Visual Analytics for Correlation-Based Comparison of Time Series Ensembles. - *Computer Graphics Forum*, *34*, 3, pp. 411—420.

DOI: http://doi.org/10.1111/cgf.12653

# Visual Analytics for Correlation-Based Comparison of Time Series Ensembles

Patrick Köthur[1,2], Carl Witt[1,2], Mike Sips[1], Norbert Marwan[3], Stefan Schinkel[3] and Doris Dransch[1,2]

[1]GFZ German Research Centre for Geosciences, Potsdam, Germany
[2]Humboldt-Universität zu Berlin, Geography Department, Berlin, Germany
[3]Potsdam Institute for Climate Impact Research, Potsdam, Germany

**Abstract**

An established approach to studying interrelations between two non-stationary time series is to compute the 'windowed' cross-correlation (WCC). The time series are divided into intervals and the cross-correlation between corresponding intervals is calculated. The outcome is a matrix that describes the correlation between two time series for different intervals and varying time lags. This important technique can only be used to compare two single time series. However, many applications require the comparison of ensembles of time series. Therefore, we propose a visual analytics approach that extends the WCC to support a correlation-based comparison of two ensembles of time series. We compute the pairwise WCC between all time series from the two ensembles, which results in hundreds of thousands of WCC matrices. Statistical measures are used to derive a concise description of the time-varying correlations between the ensembles as well as the uncertainty of the correlation values. We further introduce a visually scalable overview visualization of the computed correlation and uncertainty information. These components are combined with multiple linked views into a visual analytics system to support configuration of the WCC as well as detailed analysis of correlation patterns between two ensembles. Two use cases from very different domains, cognitive science and paleoclimatology, demonstrate the utility of our approach.

## 1 Introduction

Time series are analyzed in many scientific disciplines. An essential analysis task is the correlation-based comparison of time series. It allows for studying important phenomena such as climate impacts on the spreading of hazardous infectious diseases [15]. A powerful technique for this task is the windowed cross-correlation (WCC) [2, 5]. It addresses two frequent problems: (1) there can be a time lag between the temporal behavior in different time series [14], and (2) the time series can be non-stationary and, thus, their correlation can change over time [45]. The WCC solves these problems for the comparison of two time series as follows: It divides the time series into intervals of equal length, called windows (Fig. 1a). Then, the cross-correlation (CC) between corresponding windows is calculated (Fig. 1b). The CC shifts two windows relative to each other and computes the correlations between them for a range of temporal offsets (lags) [28]. The outcome of the WCC is a two-dimensional matrix of correlations between two time series. The columns represent the position of the time windows, the rows the different lags. A static plot of this matrix, in which correlation values are mapped to color (Fig. 1c and 1d), is typically used by scientists to investigate the time-varying correlation between two time series [29].

Although powerful, the WCC only address the comparison of two individual time series. However, many scientific disciplines such as climate modeling [6], chemistry [41], or brain research [3] study ensembles of time series (sets of time series produced, e.g., through Monte Carlo

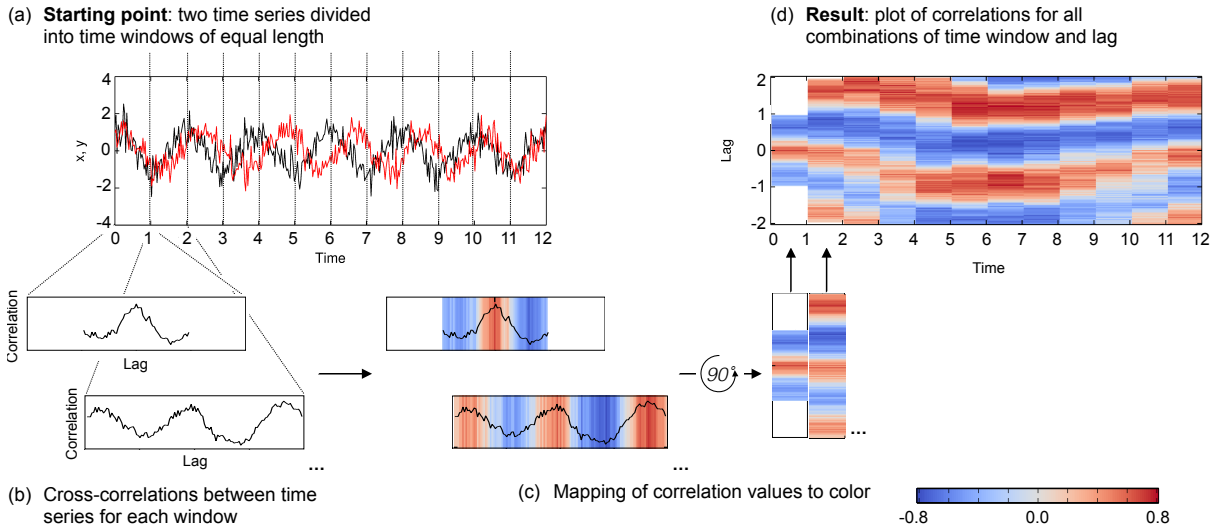


Figure 1: Computation and basic plot of the windowed cross-correlation between two time series. The time series are divided into windows of equal length (a) and the cross-correlation between the time series for corresponding intervals is calculated (b). The resulting matrix of correlations can be visualized by mapping correlation to color (c). The matrix plot shows that one time series exhibits a time-varying phase difference, visible by the change of the lagged correlation over time (d).

simulation or repeated measurements). Therefore, we extend the WCC to a visual analytics solution that supports a correlation-based comparison of two ensembles of time series. Our approach combines semiautomatic statistical analysis with interactive visual exploration. The computational part enables users to calculate the pairwise WCC between all time series from the two ensembles. Since a single ensemble may easily comprise hundreds of time series, this yields hundreds of thousands or even millions of WCC matrices. Each matrix depicts the same combinations of time window and lag; only the correlation values differ between matrices. To support visual exploration, we use statistical measures to describe the resulting distribution of correlation values at each combination of time window and lag. The outcome of the statistical analysis is presented in a visually scalable overview visualization of the WCC. It depicts the sign, magnitude and uncertainty of the time-varying correlations between two ensembles. WCC computation and overview visualization are combined with multiple linked views into a visual analytics system. It supports flexible configuration of the WCC and detailed analysis of correlation patterns as well as relating these patterns to the input ensemble data.

This approach is based on a thorough task- and requirement analysis. After an overview of related work (Section 2), we will provide more detail about the identified requirements (Section 3). To meet these requirements, we had to face a number of visualization challenges, in particular, plotting and exploring more than a thousand time series with up to 10k observations each, visualizing large WCC matrices, as well as visualization and exploration of uncertainty information. Section 4 will describe the individual components of our concept and how they address the requirements and visualization challenges. We further provide two use cases from very different domains to demonstrate the significance of our approach (Section 5): (1) detection of event-related potentials in electroencephalography (EEG) measurements and (2) comparison of paleoclimate time series ensembles derived from stalagmites. Finally, we summarize our results and suggest areas of future work (Section 6).

## 2 Related work

Since we have covered studies concerning the computation and application of the windowed cross-correlation in the introduction, we will focus this section on related work from the visualization community.

While many works support visualization and visual exploration of time series data [1], only a limited number of systems focus on the visual analysis of ensemble data [21]. These approaches provide valuable solutions for applications such as weather forecasting [37, 39], finding potential indicators of climate change [22], car engine optimization [31], or development of power train systems [35].

We address the comparison of time series ensembles, in particular, the detection of time-varying correlations between two ensembles. For exploration of the ensemble data, we took inspiration from works that use binning to visualize time series with thousands of observations [4, 9], and approaches that map line density to opacity to visualize large sets of time series at interactive frame rates [32,33]. To analyze the uncertainty of correlations between two ensembles, we studied various guidelines for encoding uncertainty information [26,27,46]. We were especially inspired by approaches that use statistical moments to visualize the uncertainty in distributions of numerical values [8, 18, 20, 34, 36, 37]. Since we must cope with a large number of distributions of correlation values, we turn to matrix visualization, which allows for displaying massive data in a compact visual overview [44]. We specifically build on a matrix visualization technique called Hinton diagram [16, 17]. This technique is used in network analysis to visualize, e.g., network weights or activations of units in a network [7, 24]. We extend the Hinton diagram to a matrix that supports hierarchical aggregation and semantic zooming [12, 13] to depict the time-varying correlations between two ensembles as well as their uncertainty.

## 3 Design requirements

The visual analytics approach presented in this article is the result of a close collaboration with two experts in time series analysis, both co-authors of this paper. A user- and task-centered approach [11] that involved frequent meetings and discussions allowed us to elicit the following design requirements for the comparison of two time series ensembles via WCC:

DR1 *Allow for flexible configuration of windowed cross-correlation (WCC) computation*

Scientists typically focus on particular aspects of correlations during the comparison of time series via WCC, such as short-, medium-, or long-term temporal variations of correlation. Each of these aspects requires a different set of parameters for the WCC computation. Furthermore, scientists sometimes want to focus the comparison on specific subsets of the ensembles. Both – analysis focus and subsets of interests – may change in the comparison process. Researchers must therefore be able to:

- Choose between comparing entire ensembles or user-specified subsets.
- Modify the parameters and recompute the WCC.
- Browse and easily access WCC results previously computed in the analysis process.

DR2 *Provide measures that capture the uncertainty of computed correlation values*

Our collaborating scientists consider the spread of a distribution of correlation values as uncertainty. They require quantitative information about this spread for each combination of time window and lag in the WCC. A common approach is to calculate statistical moments that quantify the central tendency and the degree of dispersion. These measure can then be used in (interactive) visualizations to further facilitate the assessment of uncertainties. Therefore, a visual analytics approach must:

- Provide measures of central tendency.
- Provide measures of dispersion.
- Provide confidence intervals.

DR3 *Provide overview of correlations and their uncertainty*

Scientists want to detect the predominant patterns in the correlations between two time series ensembles, especially patterns of temporal variation and patterns of uncertainty of correlation values. This requirement is associated with the following tasks:

- Obtain overview of correlation values for all combinations of time window and lag.
- Obtain overview of the uncertainty of correlation values for all combinations of time window and lag.

DR4 *Support exploration of correlations and their uncertainty*

After detecting the predominant patterns of correlation and uncertainty, researchers want to gain a detailed understanding of the time-varying correlation between two ensembles as well as the reliability of the results. To this end, they need to:

- Inspect in detail the temporal variation of correlations and the variations in uncertainty.
- Assess the statistical significance of correlation values.
- Examine the distribution of correlation values for individual combinations of time window and lag.

DR5 *Support inspection of the two time series ensembles*

To interpret the results of the WCC computation and to gain a better understanding of the time-varying correlation, scientists have to inspect and compare the ensemble data that went into the calculation. In particular, they have to:

- Obtain an overview of the time series in the two ensembles.
- Inspect and compare the distribution of time series in the ensembles.

# 4 Visual analytics approach

To meet the identified requirements, our concept combines two modules: semiautomatic statistical analysis (module M I) and interactive visual exploration[1] (module M II). Each module comprises several components (Figure 2).

## 4.1 Linking between modules and components

On a module level, users choose the ensemble data and parametrize the WCC calculation in module M I, which then computes the data for visual exploration in module M II. The insight researchers gain through interactive visual exploration may change the focus of analysis, which, in turn, may prompt users to go back and modify the WCC parameters or even the input data.

On the component level, M I.1 passes the user-selected ensemble data and the parameters for the WCC computation to M I.2. The latter calculates the pairwise WCC between the time series from both ensembles and forwards the resulting WCC data to M I.3. Component M I.3 computes statistical measures to summarize the correlations and their uncertainty. These data are passed to component M II.1 for visual exploration. This component provides researchers with

[1] A supplementary demo video of the prototype illustrating the visual exploration part can be found at `http://doi.org/10.2312/GFZ.1.5.2016.001`

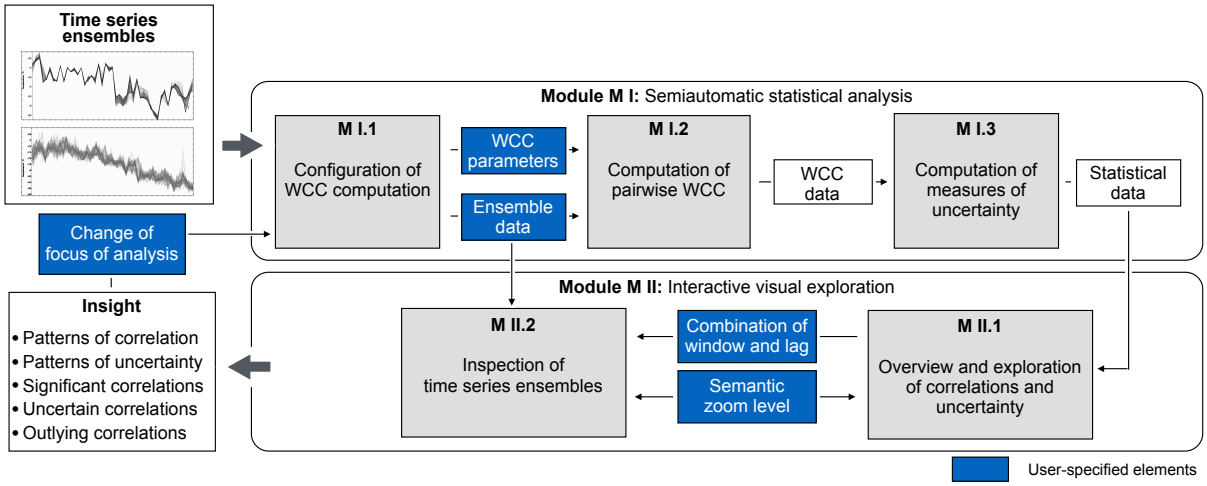


Figure 2: Our visual analytics concept. It comprises computation and statistical analysis of windowed cross-correlations (WCC) between two time series ensembles (module M I) and interactive visual exploration of the resulting time-varying correlations and their uncertainty (module M II).

an overview of the correlation results. It also allows users to interactively filter combinations of time window and lag that meet specified criteria regarding correlation values and uncertainty. The underlying distribution of correlation values for selected combinations of time window and lag can also be explored in M II.1, while the corresponding time series data can be studied in component in M II.2. Both components, M II.1 and M II.2, support hierarchical aggregation and semantic zooming to cope with the limited screen space.

The remainder of this section will describe the two main modules of our concept as well as their respective components and how they address the design requirements.

## 4.2 Module M I: Semiautomatic statistical analysis

This part comprises components M I.1, M I.2, and M I.3 which cover design requirements DR1 and DR2.

### Component M I.1: Configuration of windowed cross-correlation (WCC) computation

DR1 – *Allow for flexible configuration of WCC computation.*

Component M I.1 allows scientists to choose the two ensembles for comparison and, if need be, to further focus on particular time series from the two ensembles. Next, researchers use M I.1 to set the parameters for the WCC: window size, overlap between consecutive windows, and lag range. Scientists do not necessarily have to initiate a new computation. For every compared pair of ensembles, we store previous WCC configurations and results in a database. Scientists can use this component to browse through and to revisit them. When users decide to initiate a new computation, the ensemble data and the WCC parameters are passed to component M I.2.

### Component M I.2: Computation of pairwise of windowed cross-correlation (WCC)

This component performs the actual WCC computation. Let $M$ and $N$ be the two sets (ensembles) of time series. All time series in $M$ and $N$ must be equal regarding the number of observations, the timestamps of the observations, and the length of intervals between observations. Note that M I.2 could also be extended to include correlation analysis techniques for irregularly sampled time series, such as kernel based correlation estimation [38]. We compute

the WCC for all pairs of time series in $M \times N$ (see [5] for details regarding the computation of the WCC). As a result, we obtain $k = |M \times N|$ WCC matrices. These data are passed to component M I.3.

#### Component M I.3: Computation of measures of uncertainty

DR2 – *Provide measures that capture the uncertainty of computed correlation values.*

Since the same parameters were used for all WCC computations, each matrix depicts the same combinations of time window and lag; only the correlation values differ between matrices. Hence, we obtain a distribution of correlations for each window-lag combination. We use descriptive statistics for analyzing the uncertainty in these distributions [42]. This component calculates the mean and median correlation as measures of central tendency for each window-lag combination, and the standard deviation and interquartile range as measures of dispersion. It also determines the confidence interval of the correlations for a user-specified $p$-value with a $t$-test [42]. This information is then used to calculate the percentage of statistically significant correlations at each combination of window and lag. Note that M I.3 is not limited to this set of statistical measures. If need be, our concept allows for incorporating additional measures.

### 4.3 Module M II: Interactive visual exploration

This module is composed of component M II.1, which covers design requirement DR3 as well as DR4, and component M II.2, , which addresses design requirement DR5.

#### Component M II.1: Overview and exploration of correlations and their uncertainty

DR3 – *Provide overview of correlations and their uncertainty.*

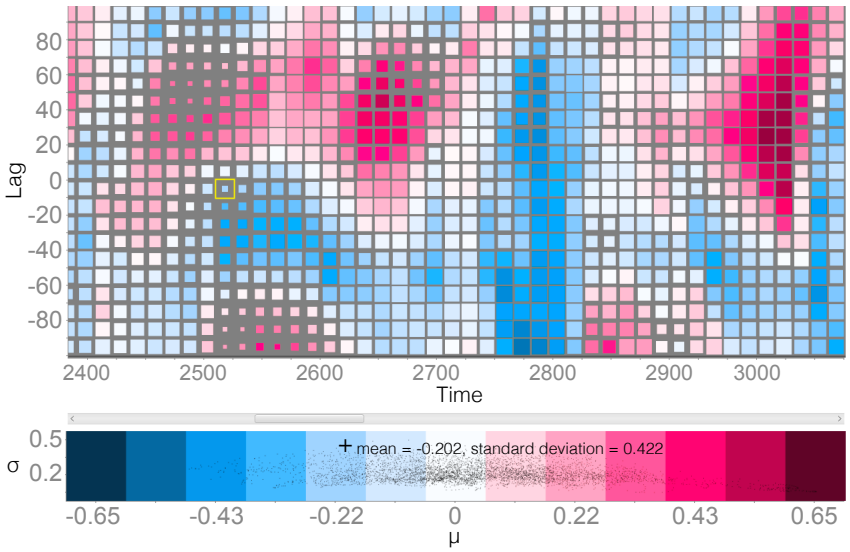


Figure 3: Correlations view (top) and color legend with integrated scatter plot (bottom) of component M II.1. The color of the squares encode the mean or median correlations of each combination of time window (x-axis) and lag (y-axis). The size inversely depicts the uncertainty of the underlying distribution. Thus, small squares represent high uncertainty. When users select a window-lag combination it is highlighted in the correlations view (yellow square) and in the scatter plot (labeled cross).

To address this requirement, we extend the basic WCC matrix plot introduced in Figure 1 to an interactive and visually scalable visualization of the WCC and its uncertainty. Our technique is inspired by Hinton diagrams [16, 17]. We map each combination of time window and lag to

a square in a matrix (Figure 3). The color of the square denotes the mean of the underlying distribution of correlation values. We use a diverging color scale to differentiate positive and negative correlations of different magnitude. It is centered around zero and its range is determined by the highest absolute correlation value in the data. The square's size inversely encodes the standard deviation of the distribution. Hence, the higher the uncertainty (or variation), the smaller the square. For more robustness against outliers, users can alternatively choose to display the median and interquartile range in the correlations view. The statistical measures for this mapping are provided by component M I.3.

The texture that results from arranging the squares on the $XY$ plane facilitates preattentive processing of patterns. This view enables scientists to differentiate strong correlations (saturated colors) from weak correlations (light colors) and uncertain values (small squares) from rather certain correlations (large squares). Note that color and size in this encoding potentially interact [10]. In our scenario, however, scientists are particularly interested in strong correlations that relatively certain. These represent the most reliable indicators of meaningful correlations between two ensembles. Since this information is emphasized in our design through large squares of intense color, there is little chance of misinterpretation.

Although Hinton diagrams are a powerful technique, they do not scale well to large WCC matrices because the squares encoding the numerical values require significant screen space. We experimented with mapping uncertainty to transparency instead of size as a more space-efficient encoding. However, this alternative hindered the interpretation of correlation values. Therefore, we chose to extend the Hinton technique to support semantic zooming [13]. We bin the matrix whenever the screen space does not suffice to display all squares. The statistical information conveyed by the squares in each bin is summarized in a single glyph. We operate on the statistical information encoded in the input squares instead of the underlying distributions of correlations because it allows for on-the-fly construction of the glyphs and, hence, zooming of the matrix in real time. The glyph is composed of three nested squares (Figure 4). The color of the middle square encodes the median correlation of the input squares; its size represents the median uncertainty. A transparent outer square denotes the uncertainty of the least uncertain input square. A transparent inner square shows the uncertainty of the most uncertain input square. We chose this design for three reasons: (1) it preserves the visual encoding of the input squares, (2) it conveys information about the range of uncertainty among the aggregated window-lag combinations, and (3) the glyphs are easily distinguishable from the squares of the non-aggregated representation, which signals to users that they are looking at visual aggregates. The binning of the matrix depends on the available screen space and the minimum sizes of the squares and glyphs. When users change the zoom level, the new binning as well as the input squares for each bin are determined, and the glyphs are adjusted accordingly.

To enable scientists to obtain an overview of potential relationships between correlation values and uncertainty across all window-lag combinations, we integrate a scatter plot into the color legend of the correlations view (Figure 3). It shows the mean or median correlation values plotted against the uncertainty. Furthermore, the correlations view and the scatter plot are linked to enable exact quantitative assessment. When users mouse-point at any window-lag combination in the matrix, the exact correlation and uncertainty values are displayed in the scatter plot.

To present scientists with additional information about the uncertainty of correlation values, our tool provides an alternative view of the WCC matrix. This view maps the fraction of statistically significant correlations at each combination of time window and lag to color in a pixel display (see Figure 10 for a view of the fraction of positive correlations).

DR4 – *Support exploration of correlations and their uncertainty.*

Besides a semantic zoom for detailed inspection of correlations and uncertainties, component M II.1 provides two additional mechanisms to meet requirement DR4.

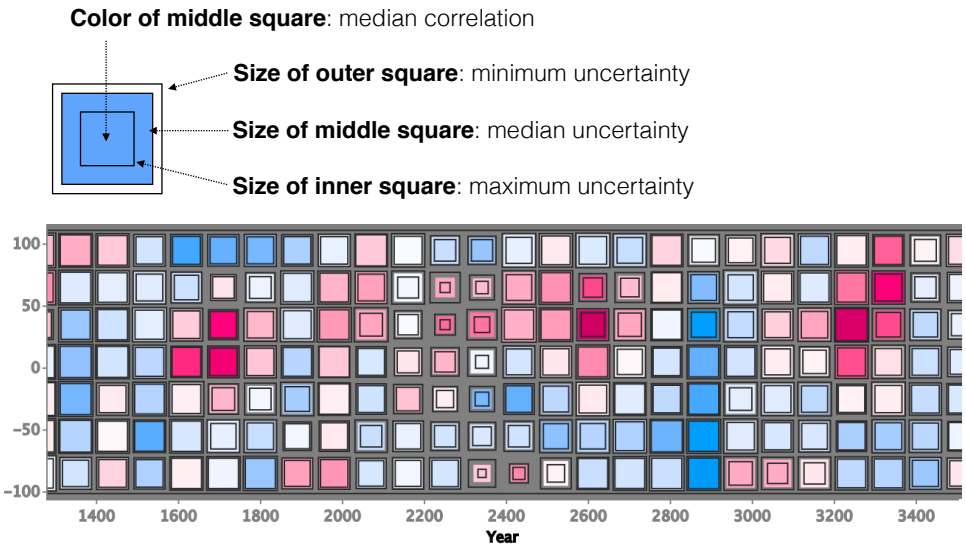


Figure 4: Glyph encoding the results of aggregating the distributions of correlations from multiple window-lag combinations (top) and a zoomed-out version of the correlations view using the glyph (bottom). 'Uncertainty' denotes either standard deviation or interquartile range of correlation values. Small squares signal high uncertainty and vice versa.

The first mechanism is interactive filtering via range sliders. Scientists can use these sliders to gray out window-lag combinations in the correlations view that do not meet specified quantitative criteria. In particular, we offer the measures from component M I.3 for filtering: mean and median correlation, standard deviation, interquartile range, and the fraction of significant (negative/positive/total) correlations at the window-lag combinations. The correlations view adjusts in real time, which allows scientists to explore the variation of correlations and their uncertainty, as well as the statistical significance of the correlations.

To enable scientists to explore the distributions of correlation values that are represented by each square in the correlations view, we provide an on-demand histogram (Figure 5). It allows researchers to examine properties of the underlying distributions, e.g., modality or symmetry. Furthermore, gray areas in the histogram mark the statistically significant portions of the distribution.

### Component M II.2: Visual inspection and comparison of the two time series ensembles

DR5 – *Support inspection of the two time series ensembles.*

Component M II.2 visualizes the two time series ensembles that went into the WCC calculation (Figure 6). Both ensembles are plotted in the same line chart with a unique color assigned to each ensemble. This facilitates inspection and comparison regarding trends, amplitude, scale, and range – valuable information that helps scientists to interpret the WCC results. Users can

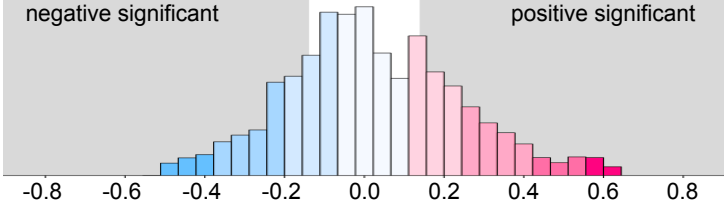


Figure 5: On-demand histogram of correlation values for a combination of time window and lag. The gray areas in the background mark statistically significant correlations.

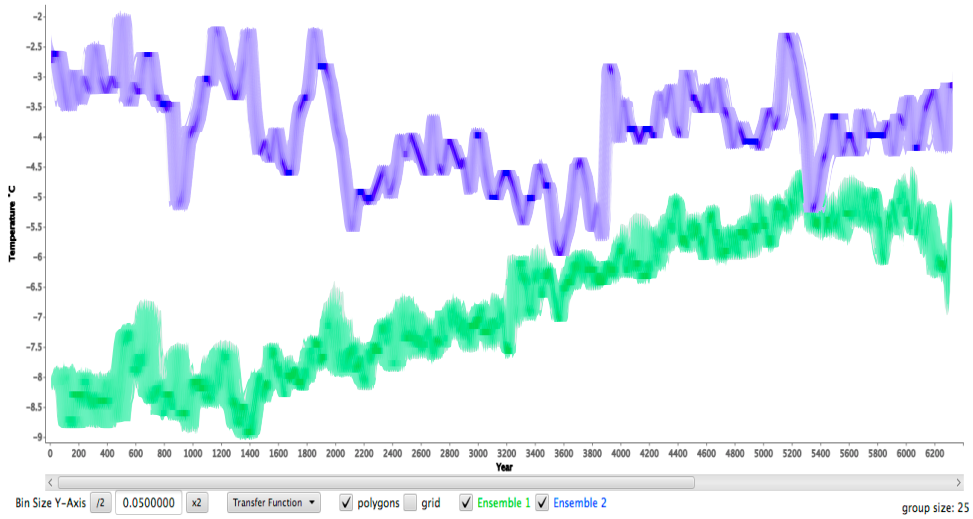


Figure 6: Line chart showing both ensembles (component M II.2). Line density is mapped to opacity to depict the uncertainty in the ensembles. Dense regions in each ensemble are mapped to high opacity, sparse regions are more transparent to indicate less agreement among ensemble members.

further choose between displaying the original time series data or normalized versions. The latter enables scientists to compare the two ensembles on the same scaling level while the former accentuates differences in scaling level.

To make M II.2 visually scalable, we had to address two issues: (1) visualization of time series with thousands of data points, and (2) depicting hundreds or thousands of time series in the same plot.

We use a binning approach in combination with semantic zooming to address the first issue. In particular, we divide the time series into intervals of equal length (bins) and calculate the mean of each interval. The resulting averaged time series are then shown in the line chart. Semantic zooming and panning enables scientists to inspect the binned time series in more detail. After each zooming action the bin size (level of aggregation) is adjusted automatically to match the number of pixels available to display the selected time range.

To address the second scalability issue, we map the line density of each ensemble to opacity [22, 32, 33]. Dense regions signal high agreement among ensemble members and are mapped to high opacity; sparse regions are more transparent to indicate less agreement among ensemble members. This provides users with an overview of the distribution of time series within the ensembles. If need be, check-boxes allow scientists to display, and therefore focus on, only one of the two ensembles.

# 5 Use cases

We demonstrate the utility of our concept with two applications from the fields of cognitive science and paleoclimatology. In both fields, ensembles of time series are frequently compared. However, the standard procedure is to compare only the mean or median time series of the ensembles. Our visual analytics approach enabled us to perform a correlation-based comparison of entire ensembles.

## 5.1 Interpersonal detection of event-related potentials

In cognitive science, the brain activity is studied by measuring the electroencephalogram (EEG) at the human scalp. In experiments, stimuli are presented to subjects and the potential changes

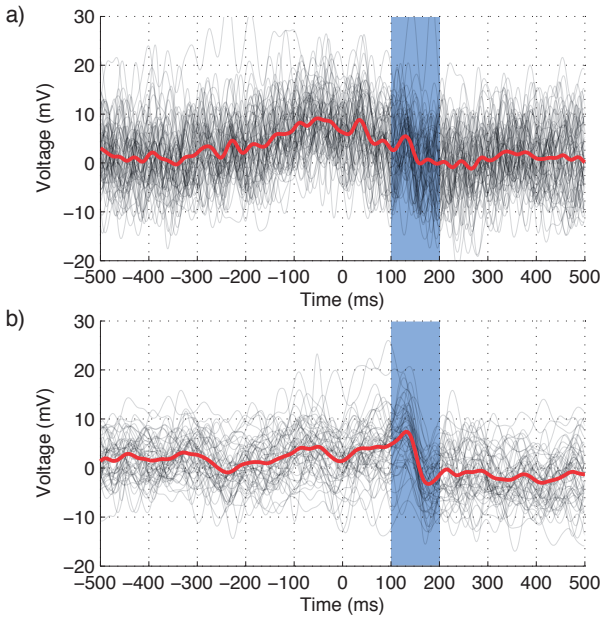


Figure 7: Electroencephalogram (EEG) ensembles of two subjects (a) and (b). The red lines represent the average of the respective trial. After a visual stimulus at time $t = 0$ ms, an evoked electrophysiological activity around 170 ms (marked by the blue shading) can be clearly observed for subject (b), but only suspected for subject (a).

in measured brain activity, called event-related potential (ERP), are investigated [25]. Due to many disturbing factors, the signal to noise ratio in the EEG measurements is very low. Therefore, the trials are repeated many times and only the average of these trials is then used to identify the ERPs [40]. However, significant information about ERPs is lost, when looking only at trial averages.

In the following, we demonstrate how our visual analytics approach was used to compare entire ensembles of EEG measurements to test the assumption that the same facial stimulus causes the same electrophysiological response in different humans. The analysis considered EEG data of an experiment in which subjects were presented with different variations of a face [40]. Two subjects were randomly selected from this experiment and the measurements from a single electrode were used to compare the interpersonal electrophysiological activity. For the first subject 66 trials and for the second subject 51 trials were available (Figure 7). The presented stimulus usually evokes a negative potential change at 170 ms, a so called N170. Analyzing the N170 provides important information about a person's sensitivity to faces. Note that while in panel (b) of Figure 7 a prototypical N170 response can be observed, this is not obvious in panel (a).

To analyze whether both subjects show similar sensitivity to faces, the pairwise WCC between their respective EEG ensembles was computed. Based on their expert knowledge, scientists considered the following parameters to be appropriate: window size of 55 ms, window overlap of 45 ms, and lag range of -25 to 25 ms. The correlations view revealed strong correlations between the ensembles in the time interval between 120 and 170 ms (Figure 8a). Inspecting individual window-lag combinations with the on-demand histogram showed that within the interval between 120 and 170 ms, the majority of the trials in the ensembles were positively correlated (Figure 8b).

Our approach clearly reveals that the subjects' responses to faces are similar. Moreover, the high correlation values between 120 and 170 ms show a tendency to be lagged by 10 ms. This suggests that subject one has a slightly slower reaction time than subject two. These insights cannot be readily inferred from the plots shown in Figure 7 or by only comparing individual

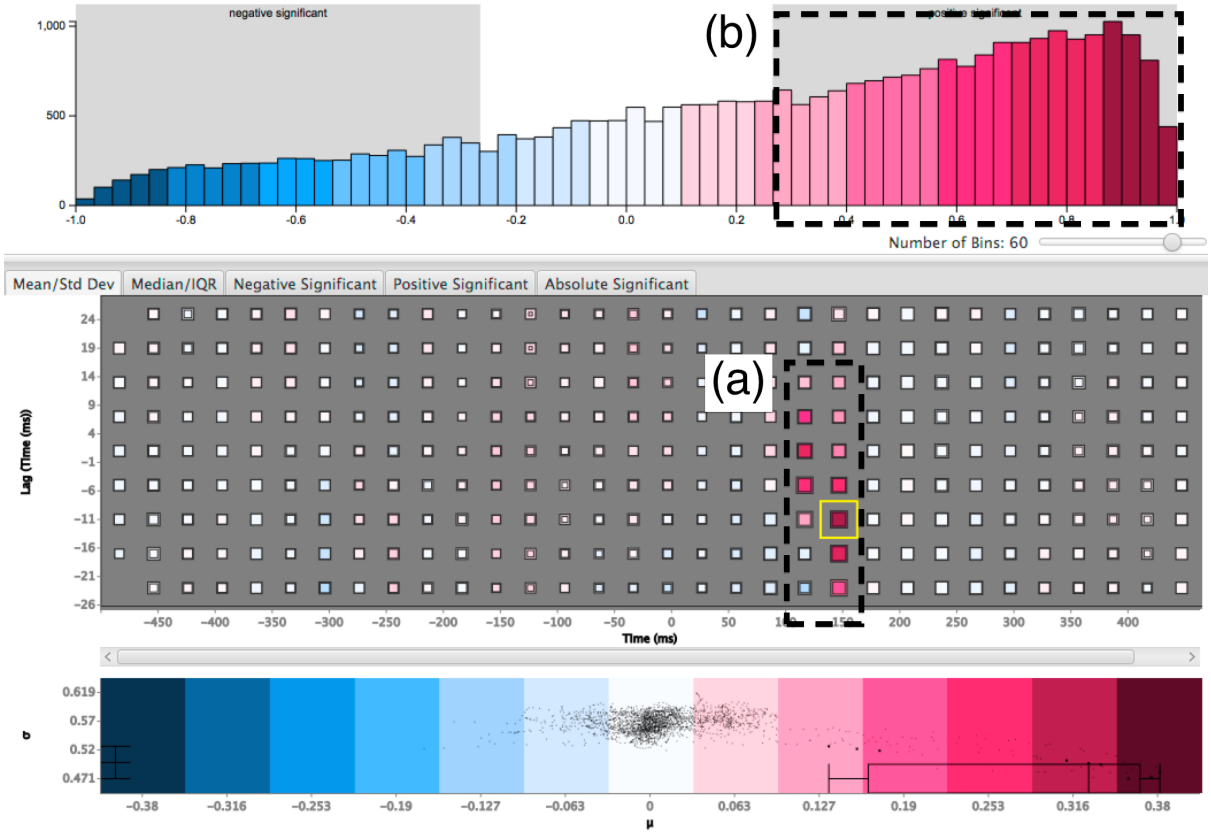


Figure 8: Correlations between EEG ensembles of two subjects. In both subjects, the presented facial stimulus causes the same electrophysiological activity between 120 and 170 ms (a). This is revealed by the strong correlations within this time interval. The histogram shows that the majority of the trials is significantly correlated (b).

trials. From these results it can be concluded that the same facial stimulus causes very similar electrophysiological activity in the two subjects.

### 5.2 Replication of paleoclimate variation derived from stalagmites

In a second example we focus on an important problem in paleoclimatology, where proxy records (such as time series derived from ice cores or stalagmites) from almost the same location would be expected to represent a similar behavior. This is called replication of proxy records and is often not the case, because either the proxies are not reflecting the paleoclimate variation or external factors dominate the climate signal in the proxy record [19, 23].

The comparison involves two proxy records derived from stalagmites collected in Heshang cave [19] and Sanbao cave [43], both located in China. Both records cover the period between 9000 years before present (BP) and 500 years BP. The caves are quite close (approximately 150 km) and the two proxy records should reproduce the same climate signal. The dating of the proxy records involves a certain amount of uncertainty. Therefore, a Monte Carlo approach was used to create ensembles of possible realizations of time series [6].

To analyze the replication, the WCC between both proxy record ensembles was envestigated with our visual analytics approach. A typical time scale of interest to paleoclimatologists is 500 years, with an overlap of 430 years. Since the dating uncertainty in these particular ensembles is up to 200 years, a lag range of $\pm 200$ years was chosen. Our tool reveals correlations between both ensembles for the entire time period (Figure 9). The varying magnitude and uncertainty of correlations uncovers significant variation in the ensembles. This variation, which is also visible


Figure 9: The windowed cross-correlation between two ensembles of paleoclimate time series. In accordance with domain-specific conventions, the most recent observations are plotted on the left and the oldest on the right.

in the time series view (Figure 9 top), is caused by dating uncertainties. Studying the fractions of significant positive correlations over all combinations of time window and lag (Figure 10) reveals the generally strong correlation between both ensembles. This particular visualization provides valuable information that allows for reducing the dating uncertainties by extracting a correction function that aligns both proxy records to the same chronology. Note that for some epochs, e.g., around 7700 years BP, the fraction of significant correlations is high over a range of lags (dashed rectangle in Figure 10). To identify a suitable lag for a correction function, the distributions at the corresponding window-lag combinations were compared. The most suitable lag is the one that has the largest number of high positive correlation values. For example, for the time period at 7700 years BP, the highest correlation values can be found at lag −80 (Figure 10(b)), whereas at other lags the number of high, though still significant, correlation values is reduced (Figure 10(c, d)).

From these findings it can be concluded that both proxy records replicate well, although not perfectly. Main issues are differences between the records caused by unresolved processes influencing the dating procedure. However, the proposed visual analytics approach enabled the extraction of a correction function which reduces the uncertainties in the dating procedure.

## 6 Summary and conclusion

In this paper, we presented a visual analytics approach that extends an established method for correlation-based comparison of two time series – windowed cross-correlation – to support

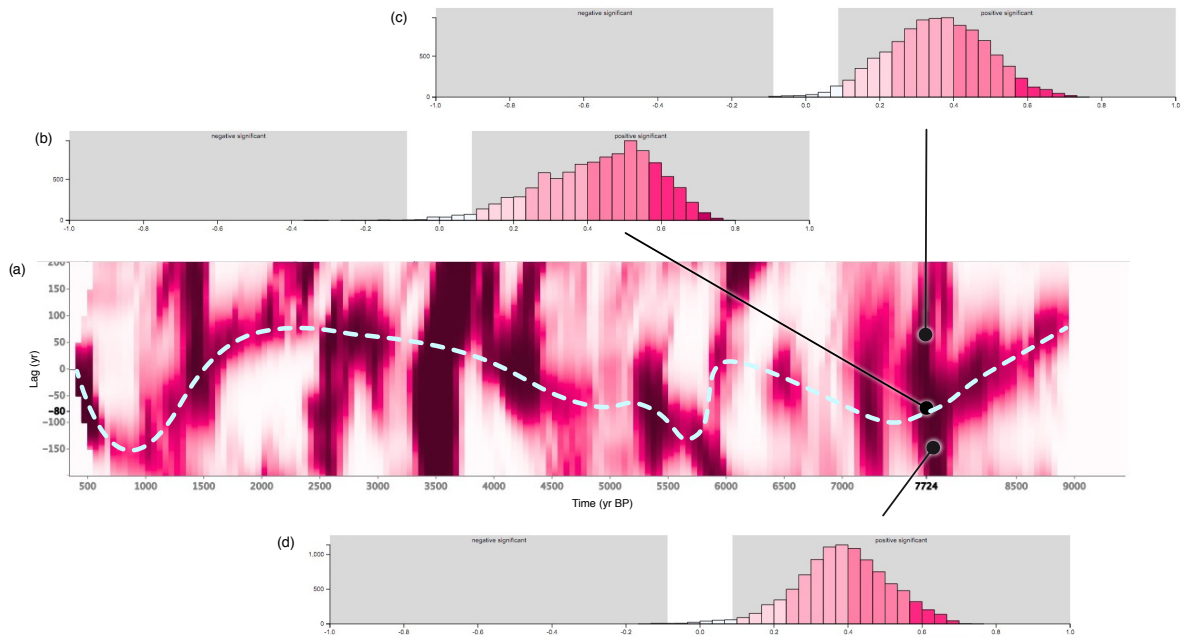


Figure 10: (a) Fractions of significant positive correlations between two ensembles of paleoclimate time series. The dashed line indicates the derived correction function for reducing the dating uncertainties. (b–d) Looking at the distributions of correlation values for different lags at the epoch around 7700 years BP (dashed rectangle) allows for identifying the most suitable lag for the correction function. Since (b) exhibits the largest portion of high correlations, its respective lag was chosen.

the comparison of entire ensembles of time series. To meet the requirements of time series analysts, we combined semiautomatic statistical analysis with visual exploration in a field-ready visual analytics system. We further build on Hinton diagrams to derive a novel visualization of windowed cross-correlations between ensembles. This matrix-like visualization is visually scalable through semantic zooming and provides an overview of the magnitude and uncertainty of the time-varying correlations between two ensembles. Two use cases demonstrated that our concept allows for gaining valuable insight into the interrelations between ensembles of time series. Insight which, according to the co-authoring domain experts, could only be obtained with our approach.

Regarding the performance of our system, one has to consider two aspects: the computation of the WCC and the statistical measures, and the interactive visual exploration. The run time of the former highly depends on the application scenario, i.e., the number of time series, the number of observations per time series, and the parameters of the WCC. In the two use cases (Section 5), the WCC calculation took 3 and 37 seconds, respectively (2.6 GHz Intel Core i5 laptop). Since our tool is for domain experts who typically know the appropriate parameters, the computational cost of the WCC calculation was not a concern in our scenarios. The subsequent visual analysis is highly interactive, allowing for real-time exploration of the computed correlations.

To address an even wider range of analysis tasks, we plan two extensions of our approach. (1) Since our concept is also applicable to other methods for studying interrelations between time series, e.g., cross and joint recurrence [14, 30], we intend to incorporate these methods. (2) We would also like to support the comparison of more than two ensembles, adapting our concept to the visual analysis challenges posed by a multi-way comparison.

## Acknowledgements

This research was in part funded by the German Federal Ministry of Education and Research (BMBF project PROGRESS, 03IS2191B).

## References

[1] W. Aigner, S. Miksch, H. Schumann, and C. Tominski. *Visualization of time-oriented data*. Springer, 2011.

[2] U. Altmann. Investigation of movement synchrony using windowed cross-lagged regression. In A. Esposito, A. Vinciarelli, K. Vicsi, C. Pelachaud, and A. Nijholt, editors, *Analysis of Verbal and Nonverbal Communication and Enactment. The Processing Issues*, volume 6800 of *LNCS*, pages 335–345. Springer, Berlin Heidelberg, 2011.

[3] E. Başar, C. Başar-Eroglu, R. Parnefjord, E. Rahn, and M. Schürmann. Evoked potentials: Ensembles of brain induced rhythmicities in the alpha, theta and gamma ranges. In E. Başar and T. H. Bullock, editors, *Induced Rhythms in the Brain*, Brain Dynamics, pages 155–181. Birkhäuser, Boston, 1992.

[4] L. Berry and T. Munzner. Binx: Dynamic exploration of time series datasets across aggregation levels. In *IEEE Symposium on Information Visualization, 2004*. IEEE, Oct 2004.

[5] S. M. Boker, J. L. Rotondo, M. Xu, and K. King. Windowed cross-correlation and peak picking for the analysis of variability in the association between behavioral time series. *Psychol. Methods*, 7(3):338–355, 2002.

[6] S. F. M. Breitenbach, K. Rehfeld, B. Goswami, J. U. L. Baldini, H. E. Ridley, D. Kennett, K. Prufer, V. V. Aquino, Y. Asmerom, V. J. Polyak, H. Cheng, J. Kurths, and N. Marwan. Constructing Proxy-Record Age models (COPRA). *Clim. Past*, 8:1765–1779, 2012.

[7] F. J. Bremner, S. J. Gotts, and D. L. Denham. Hinton diagrams: Viewing connection strengths in neural networks. *Behav. Res. Meth. Ins. C.*, 26(2):215–218, 1994.

[8] A. Cedilnik and P. Rheingans. Procedural annotation of uncertain information. In T. Ertl, B. Hamann, and A. Varshney, editors, *Visualization 2000: October 8 - 13, 2000, Salt Lake City, UT, USA*, pages 77–83. IEEE, Piscataway, NJ, USA, 2000.

[9] R. Dachselt, M. Frisch, and M. Weiland. Facetzoom: A continuous multi-scale widget for navigating hierarchical metadata. In *Proc. SIGCHI Conf. on Human Factors in Computing Systems*, CHI '08, pages 1353–1356, New York, NY, USA, 2008. ACM.

[10] L. De Grandis. *Theory and use of color*. Abrams, 1986.

[11] D. Dransch, P. Köthur, S. Schulte, V. Klemann, and H. Dobslaw. Assessing the quality of geoscientific simulation models with visual analytics methods – a design study. *International Journal of Geographical Information Science*, 24(10):1459–1479, 2010.

[12] N. Elmqvist, T.-N. Do, H. Goodell, N. Henry, and J.-D. Fekete. Zame: Interactive large-scale graph visualization. In *Proc. PacificVIS '08*, pages 215–222. IEEE, March 2008.

[13] N. Elmqvist and J.-D. Fekete. Hierarchical aggregation for information visualization: Overview, techniques, and design guidelines. *IEEE T. Vis. Comput. Gr.*, 16(3):439–454, May 2010.

[14] B. Goswami, N. Marwan, G. Feulner, and J. Kurths. How do global temperature drivers influence each other? – A network perspective using recurrences. *Eur. Phys. J. – Special Topics*, 222:861–873, 2013.

[15] M. Hashizume, T. Terao, and N. Minakawa. The Indian Ocean Dipole and malaria risk in the highlands of western Kenya. *Proc. NAS USA*, 106(6):1857–62, 2009.

[16] G. E. Hinton, J. L. McClelland, and D. E. Rumelhart. Distributed representations. In D. E. Rumelhart, J. L. McClelland, and the PDP Research Group, editors, *Parallel Distributed Processing: Explorations in the Microstructure of Cognition*, volume 1, pages 77–109. MIT Press, Cambrige, MA, 1986.

[17] G. E. Hinton and T. J. Sejnowski. Learning and relearning in boltzmann machines. In D. E. Rumelhart, J. L. McClelland, and the PDP Research Group, editors, *Parallel Distributed Processing: Explorations in the Microstructure of Cognition*, volume 1, pages 282–317. MIT Press, Cambrige, MA, 1986.

[18] T. Höllt, A. Magdy, P. Zhan, G. Chen, G. Gopalakrishnan, I. Hoteit, C. D. Hansen, and M. Hadwiger. Ovis: A framework for visual analysisof ocean forecast ensembles. *IEEE Transactions on Visualization and Computer Graphics*, 20(8):1114–1126, 2014.

[19] C. Hu, G. M. Henderson, J. Huang, S. Xie, Y. Sun, and K. R. Johnson. Quantification of Holocene Asian monsoon rainfall from spatially separated cave records. *Earth Planet. Sc. Lett.*, 266(3-4):221–232, 2008.

[20] D. Kao, J. L. Dungan, and A. T. Pang. Visualizing 2D Probability Distributions from EOS Satellite Image-Derived Data Sets: A Case Study. In *Visualization 2001: 21-26 October, San Diego, CA, USA*, pages 457–460. IEEE, 2001.

[21] J. Kehrer and H. Hauser. Visualization and visual analysis of multifaceted scientific data: A survey. *IEEE Transactions on Visualization and Computer Graphics*, 19(3):495–513, March 2013.

[22] J. Kehrer, F. Ladstädter, P. Muigg, H. Doleisch, A. Steiner, and H. Hauser. Hypothesis Generation in Climate Research with Interactive Visual Data Exploration. *IEEE Transactions on Visualization and Computer Graphics*, 14(6):1579–1586, Nov 2008.

[23] M. S. Lachniet. Climatic and environmental controls on speleothem oxygen-isotope values. *Quaternary Sci. Rev.*, 28:412–432, 2009.

[24] C. Lange-Küttner. Ebbinghaus simulated: Just do it 200 times. In *IEEE Int. Conf. on Development and Learning (ICDL) 2011*, volume 2, pages 1–6. IEEE, Aug 2011.

[25] S. J. Luck. *An introduction to the event-related potential technique.* MIT Press, Cambridge, 2005.

[26] A. M. MacEachren. Visualizing uncertain information. *Cartographic Perspectives*, 13:10–19, 1992.

[27] A. M. MacEachren, A. Robinson, S. Hopper, S. Gardner, R. Murray, M. Gahegan, and E. Hetzler. Visualizing Geospatial Information Uncertainty: What We Know and What We Need to Know. *Cartography and Geographic Information Science*, 32(3):139–160, 2005.

[28] H. Madsen. *Time Series Analysis.* Chapman & Hall/CRC texts in statistical science. Chapman & Hall/CRC, Boca Raton, 2008.

[29] N. Marwan. Windowed cross correlation (corrgram). MATLAB Central File Exchange, June 2007.

[30] N. Marwan and J. Kurths. Nonlinear analysis of bivariate data with cross recurrence plots. *Phys. Lett. A*, 302(5–6):299–307, 2002.

[31] K. Matković, D. Gračanin, M. Jelović, A. Ammer, A. Lež, and H. Hauser. Interactive visual analysis of multiple simulation runs using the simulation model view: Understanding and tuning of an electronic unit injector. *IEEE Transactions on Visualization and Computer Graphics*, 16(6):1449–1457, Nov 2010.

[32] P. Muigg, J. Kehrer, S. Oeltze, H. Piringer, H. Doleisch, B. Preim, and H. Hauser. A four-level focus+context approach to interactive visual analysis of temporal features in large scientific data. *Computer Graphics Forum*, 27(3):775–782, May 2008.

[33] M. Novotnỳ and H. Hauser. Outlier-preserving focus+context visualization in parallel coordinates. *IEEE Transactions on Visualization and Computer Graphics*, 12(5):893–900, Sept 2006.

[34] A. T. Pang, C. M. Wittenbrink, and S. K. Lodha. Approaches to uncertainty visualization. *Visual Computer*, 13(8):370–390, 1997.

[35] H. Piringer, S. Pajer, W. Berger, and H. Teichmann. Comparative visual analysis of 2d function ensembles. *Computer Graphics Forum*, 31(3pt3):1195–1204, 2012.

[36] K. Potter, J. Kniss, R. Riesenfeld, and C. R. Johnson. Visualizing Summary Statistics and Uncertainty. In G. Melançon, T. Munzner, and D. Weiskopf, editors, *Eurographics/IEEE-VGTC Symp. Visualization 2010: 9-11 June 2010, Bordeaux, France*, pages 823–832. Blackwell, Oxfor, UK, 2010.

[37] K. Potter, A. Wilson, P.-T. Bremer, D. Williams, C. Doutriaux, V. Pascucci, and C. R. Johnson. Ensemble-Vis: A Framework for the Statistical Visualization of Ensemble Data. In *Proc. ICDMW '09, 6 Dec 2009, Miami, Florida*, pages 233–240. IEEE, Los Alamitos and CA, 2009.

[38] K. Rehfeld, N. Marwan, J. Heitzig, and J. Kurths. Comparison of correlation analysis techniques for irregularly sampled time series. *Nonlinear Proc. Geoph.*, 18(3):389–404, 2011.

[39] J. Sanyal, S. Zhang, J. Dyer, A. Mercer, P. Amburn, and R. J. Moorhead. Noodles: A Tool for Visualization of Numerical Weather Model Ensemble Uncertainty. *IEEE Transactions on Visualization and Computer Graphics*, 16(6):1421–1430, 2010.

[40] S. Schinkel, G. Ivanova, J. Kurths, and W. Sommer. Modulation of the N170 adaptation profile by higher level factors. *Biol. Psychol.*, 97:27–34, 2014.

[41] E. I. Shakhnovich and A. M. Gutin. Engineering of stable and fast-folding sequences of model proteins. *Proc. NAS*, 90(15):7195–7199, 1993.

[42] T. C. Urdan. *Statistics in Plain English*. Routledge, New York, London, 3rd edition, 2010.

[43] Y. Wang, H. Cheng, R. L. Edwards, X. Kong, X. Shao, S. Chen, J. Wu, X. Jiang, X. Wang, and Z. An. Millennial- and orbital-scale changes in the East Asian monsoon over the past 224,000 years. *Nature*, 451(7182):1090–3, 2008.

[44] H.-M. Wu, S. Tzeng, and C.-h. Chen. Matrix visualization. In C. Chun-houh, W. K. Härdle, and A. Unwin, editors, *Handbook of Data Visualization*, Springer Handbooks Comp. Statistics, pages 681–708. Springer, Berlin, Heidelberg, 2008.

[45] L. Zubair, G. N. Galappaththy, H. Yang, J. Chandimala, Z. Yahiya, P. Amerasinghe, N. Ward, and S. J. Connor. Epochal changes in the association between malaria epidemics and El Niño in Sri Lanka. *Malaria J.*, 7(1):140, 2008.

[46] T. D. Zuk. *Visualizing Uncertainty.* PhD thesis, University of Calgary, Canada, 2008. AAINR38246.